

Open charm hadron production via hadronic decays at STAR

David Tlustý for the STAR collaboration

^aNuclear Physics Institute, Academy of Sciences Czech Republic, Na Truhlářce 39/64, 180 86 Praha 8, Czech Republic

^bCzech Technical University in Prague, Faculty of Nuclear Sciences and Physical Engineering, Břehová 7, 11519, Prague 1, Czech Republic

Abstract

In this article, we report on the STAR results of open charm hadron production at mid-rapidity in $p + p$ and Au+Au collisions at $\sqrt{s_{NN}} = 200$ GeV and $p + p$ collisions at $\sqrt{s} = 500$ GeV. The measurements cover transverse momentum range from 0.6 to 6 GeV/c for $p + p$ 200 GeV collisions, from 1 to 6 GeV/c for $p + p$ 500 GeV collisions and from 0 to 6 GeV/c for Au+Au 200 GeV collisions. D^0 nuclear modification factor and elliptic flow in Au+Au collisions at $\sqrt{s_{NN}} = 200$ GeV are presented.

1. Introduction

The heavy quark production at RHIC is dominated by initial gluon fusion at initial hard partonic collisions and can be described by perturbative QCD (pQCD) due to their large mass [1]. The heavy constituent quark mass is almost exclusively generated through its coupling to the Higgs field in the electroweak sector, while masses of (u, d, s) quarks are dominated by spontaneous breaking of chiral symmetry (CS) in QCD [2]. This means that charm quarks remain heavy even if CS is restored, as it likely is in a QGP. One expects therefore that charm production total cross section $\sigma_{c\bar{c}}^{NN}$ should scale as a function of number-of-binary-collisions N_{bin} . In addition, if charm quarks participate in the collective expansion of the medium, there must have been enough interactions to easily thermalize light quarks. Hence, charm quark is an ideal probe to study early dynamics in high-energy nuclear collisions.

2. Analysis Method and Datasets

Invariant yield of charm quark production $\text{Inv}Y$ is calculated as

$$\text{Inv}Y \equiv \frac{d^2 N_{c\bar{c}}}{2\pi p_T dp_T dy} = \frac{1}{N_{\text{trig}}} \frac{Y(p_T, y)}{2\pi p_T \Delta p_T \Delta y} \frac{f_{\text{trg}}}{\text{BR} f_{\text{frag}} \epsilon_{\text{rec}}} \quad (1)$$

where N_{trig} is the total number of triggered events used for the analysis. $Y(p_T, y)$ is the raw charm hadron signal in each p_T bin within a rapidity window $\Delta y = 2$. BR is the hadronic decay branching ratio for the channel of interest. ϵ_{rec} is the reconstruction efficiency including geometric acceptance, track selection efficiency, PID efficiency, and analysis cut efficiency. f_{frag} represents the the ratio of charm quarks hadronized to open charm mesons. And f_{trg} is the correction factor to account for the bias between the minimum-bias sample used in this analysis and the total NSD sample [3]. f_{trg} is found to be unity in Au+Au, 0.65 in $p + p$ collisions at $\sqrt{s} = 200$ GeV and 0.58 in $p + p$ collisions at $\sqrt{s} = 500$ GeV.

$Y(p_T, y)$ is obtained from fitting the reconstructed invariant mass spectrum (Fig. 1) of open charm mesons through hadronic decays:

- 24 • $D^0(\overline{D}^0) \rightarrow K^\mp \pi^\pm$ (BR = 3.89%)
- 25 • $D^{*\pm} \rightarrow D^0(\overline{D}^0)\pi^\pm$ (BR = 67.7%) $\rightarrow K^- \pi^+ \pi^\pm$ (total BR = 2.63%)

26 The identification of daughter particles is done in the STAR experiment [5] at mid-rapidity
 27 $|y| < 1$ at $\sqrt{s_{NN}} = 200$ and 500 GeV. The analysis presented herein is done using three datasets;
 28 the first one collected in year 2009 ($N_{\text{trig}} \sim 105$ million 200 GeV p+p collisions), the second one
 29 collected in 2010 and 2011 ($N_{\text{trig}} \sim 800$ million Au+Au 200 GeV collisions), and the third one
 30 in 2011 ($N_{\text{MB}} \sim 50$ million 500 GeV p+p collisions).

31 At present, STAR does not have the capability to reconstruct the secondary vertex of D^0
 32 decay; one must calculate the invariant mass of all $K\pi$ pairs coming from the vicinity of the
 33 primary vertex. This results in a large combinatorial background which was reconstructed via
 34 the mixed-event method (Au+Au dataset), same-charge-sign, and kaon momentum-rotation ($p +$
 35 p dataset) and subtracted from invariant mass spectra of all particle pairs [6]. To reconstruct
 36 D^* , one may exploit the softness of $D^* \rightarrow D^0\pi$ decay; combine low momentum pions with
 37 D^0 candidates, i.e. pairs with $1.82 < M(K\pi) < 1.9$ GeV/ c^2 , and plot difference $M(K\pi\pi) -$
 38 $M(K\pi)$ whose resolution is determined by mostly the soft pion high momentum resolution. The
 39 combinatorial background is reconstructed by side-band (picking $K\pi$ pair outside the D^0 mass
 40 region) and wrong-sign (picking soft pion with opposite charge) methods. The dominant source
 41 of systematic uncertainties for both D^0 and D^* analyses is the difference between yields obtained
 42 from subtractions of combinatorial background from all particle combinations.

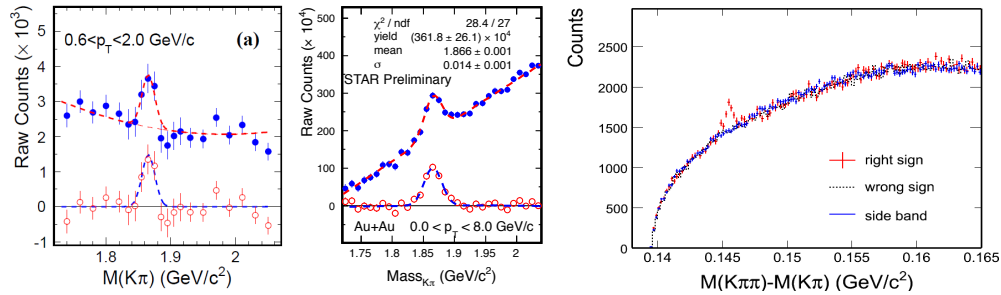


Figure 1: Left panel: D^0 signal in p+p 200 GeV collisions after same-sign background subtraction [3]. Middle panel: D^0 signal in Au+Au 200 GeV collisions after mixed-event background subtraction. Right panel: D^* signal in p + p 200 GeV collisions with combinatorial background reproduced by wrong-sign and side-band methods [3].

43 3. Results

44 3.1. D meson production in $p + p$ collisions

45 Yields $Y(p_T, y)$ are calculated in six p_T bins (first two for D^0 , the next four for D^*) in $p+p$ 200
 46 GeV and five p_T bins (first for D^0 , the next four for D^*) in $p+p$ 500 GeV. The charm cross section
 47 at mid-rapidity $d\sigma^{c\bar{c}}/dy$ was obtained from power-law function ¹ fit to $d^2\sigma^{c\bar{c}}/(2\pi p_T dp_T dy) =$
 48 $\text{Inv}Y \cdot \sigma_{\text{NSD}}$, where $\text{Inv}Y$ is obtained from (1). σ^{NSD} is the total Non-single Diffractive (NSD)
 49 cross section, which is measured at STAR to be 30.0 ± 2.4 mb at $\sqrt{s} = 200$ GeV [7]. In the
 50 case of $\sqrt{s} = 500$ GeV, there's no STAR measurement yet; σ^{NSD} is extrapolated from 200
 51 GeV measurement with the help of PYTHIA simulation to be 34 mb. The charm production

¹ $\frac{1}{2\pi p_T} \frac{d^2\sigma^{c\bar{c}}}{dp_T dy} = 4 \frac{d\sigma^{c\bar{c}}}{dy} \frac{(n-1)(n-2)}{\langle p_T \rangle^2 (n-3)^2} \left(1 + \frac{2p_T}{\langle p_T \rangle (n-3)}\right)^{-n}$

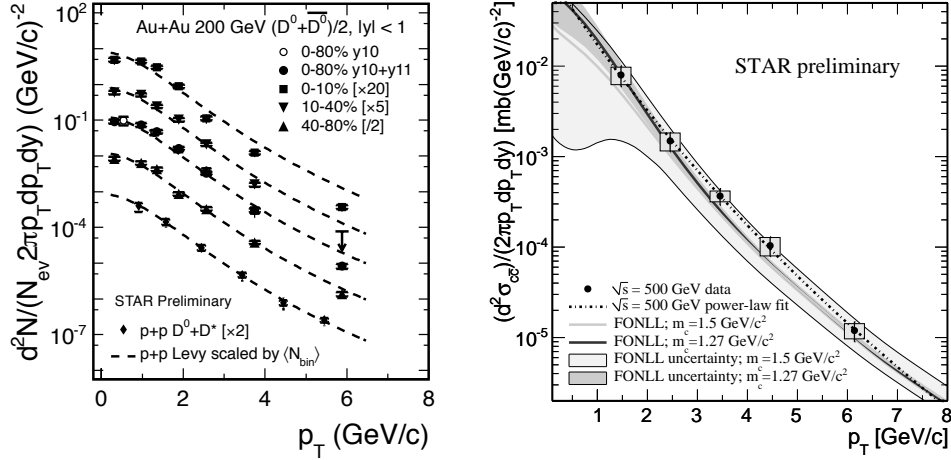


Figure 2: Left Panel: D^0 InvY spectra for various centralities, The last four p_T bins in $p + p$ collisions are from D^{*+} . Right Panel: Charm quark production invariant cross section as a function of D meson p_T in 500 GeV $p+p$ collisions with two FONLL predictions [8] using normalization and factorization scale equal to charm quark mass m_c .

52 cross section at mid rapidity $\left. \frac{d\sigma_{c\bar{c}}}{dy} \right|_{y=0}$ is $170 \pm 45(\text{stat.})_{-51}^{+37}(\text{sys.}) \mu\text{b}$ at $\sqrt{s} = 200$ GeV and is
 53 $217 \pm 86(\text{stat.}) \pm 73(\text{sys.}) \mu\text{b}$ at $\sqrt{s} = 500$ GeV. FONLL predictions for p_T spectra [8] shown in
 54 Fig. 2.

55 3.2. D^0 production in Au+Au collisions

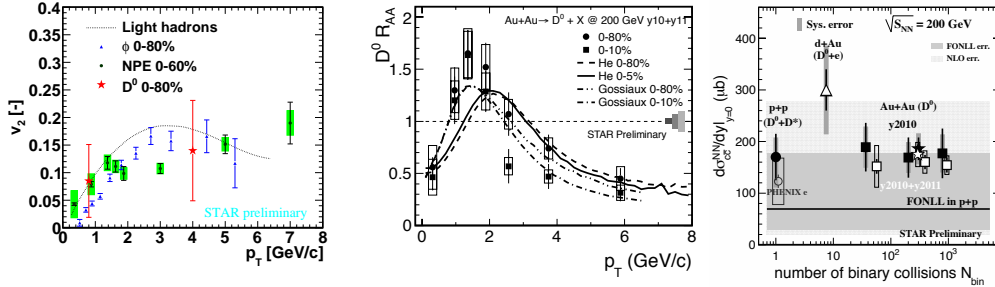


Figure 3: Left Panel: Elliptic flow as a function of p_T . Middle panel: D^0 nuclear modification factor R_{AA} as a function of p_T for most central (blue) and minimum-bias (red) Au+Au collisions with theoretical predictions from two models [10, 11]. Green rectangles around unity represent systematic uncertainties, from left to right, N_{bin} definition uncertainty for the most central (2.8%), N_{bin} definition uncertainty for all Au+Au (7%), and $p + p$ normalization error (8.1%). Right panel: The charm production cross section per N_{bin} as a function of N_{bin} .

56 Yields $Y(p_T, y)$ were calculated in eight p_T and three centrality bins. $d\sigma_{c\bar{c}}^{\text{NN}}/dy$ was obtained
 57 from the integral of

$$d^2\sigma_{c\bar{c}}^{\text{NN}}/(2\pi p_T dp_T dy) = \text{InvY} \cdot \sigma^{\text{inel}}/N_{\text{bin}} \quad (2)$$

58 over p_T and is measured to be $\left. \frac{d\sigma_{c\bar{c}}}{dy} \right|_{y=0} = 175 \pm 13(\text{stat.}) \pm 23(\text{sys.}) \mu\text{b}$. InvY is obtained from (1)
 59 and $\sigma^{\text{inel}} = 42$ mb is the total inelastic cross section [9]. To calculate the D^0 nuclear modification
 60 factor R_{AA} in various centrality bins, we scaled Levy function ² fit to $p + p$ data by N_{bin} , as shown

² $\frac{1}{2\pi p_T} \frac{d^2\sigma_{c\bar{c}}}{dp_T dy} = \frac{d\sigma_{c\bar{c}}}{dy} \frac{(n-1)(n-2)}{2\pi n C [nC + m_0(n-2)]} \left(1 + \frac{\sqrt{p_T^2 + m_0^2} - m_0}{nC} \right)^{-n}$

61 in the left panel of Fig. 2, and follow the same process for the original power-law function as
 62 discussed in section 3.1. Since enhanced statistics allow more p_T bins in Au+Au collisions, we
 63 rely on the extrapolation from the two fits to estimate one source of systematic uncertainty. The
 64 $p + p$ baseline for R_{AA} calculation is the arithmetic average of the Levy and the power-law fit
 65 results. The measurement, shown in the middle panel of Fig. 3, reveals strong suppression in
 66 the most central collisions for $p_T > 2$ GeV/c consistent with the prediction of the SUBATECH
 67 group (Gossiaux) model [11] and exhibits the maximum of the R_{AA} around $p_T \simeq 1.5$ GeV/c.
 68 This agreement with [11] might indicate that the maximum is induced by the transverse flow
 69 picked up from the expanding medium through coalescence with light-quarks.

70 $d\sigma_{cc}^{NN}/dy|_{y=0}$ as a function of N_{bin} is shown in the right panel of Fig. 3. Within errors, the
 71 results are in agreement and follow the number-of-binary-collisions scaling, which indicates that
 72 charm quark is produced via initial hard scatterings at early stage of the collisions at RHIC.
 73 The FONLL (darker band) and NLO [12] (lighter band) uncertainties are also shown here for
 74 comparison.

75 In the Left panel of Fig. 3, the measurement of D^0 elliptic flow v_2 is shown. Within large
 76 statistical error bars, D^0 v_2 is consistent with the STAR Non-photonic electrons v_2 indicating non
 77 zero elliptic flow of D^0 mesons in Au+Au collisions at $\sqrt{s_{NN}} = 200$ GeV.

78 4. CONCLUSIONS

79 New open charm hadrons (D^0, D^{*+}) measurements in $p + p$ and Au+Au minimum bias
 80 collisions at $\sqrt{s_{NN}} = 200$ GeV from STAR shows the N_{coll} scaling of the charm quark pro-
 81 duction cross section at mid rapidity. $d\sigma_{cc}^{NN}/dy|_{y=0} = 170 \pm 45(\text{stat.})_{-51}^{+37}(\text{sys.}) \mu\text{b}$ in $p + p$,
 82 $175 \pm 13(\text{stat.}) \pm 23(\text{sys.}) \mu\text{b}$ in Au+Au collisions at 200 GeV and $217 \pm 86(\text{stat.}) \pm 73(\text{sys.}) \mu\text{b}$
 83 in $p + p$ collisions at 500 GeV.

84 The new D^0 nuclear modification factor R_{AA} measurement reveals strong suppression in the
 85 most central collisions for $p_T > 2$ GeV/c consistent with the prediction of the model [11] and
 86 exhibits the maximum of the R_{AA} around $p_T \simeq 1.5$ GeV/c.

87 In the near future the STAR Heavy Flavor Tracker [13] will provide the necessary resolution
 88 to reconstruct secondary vertices of charm mesons, which will increase the precision of charm
 89 measurements.

90 Acknowledgments

91 This work was supported by grant INGO LA09013 of the Ministry of Education, Youth and Sports
 92 of the Czech Republic, and by the Grant Agency of the Czech Technical University in Prague, grant No.
 93 SGS10/292/OHK4/3T/14.

94 References

- 95 [1] M. Cacciari, P. Nason and R. Vogt, Phys. Rev. Lett. **95**, 122001 (2005).
 96 [2] X. Zhu, *et al.*, PLB **647**, 366 (2007).
 97 [3] L. Adamczyk *et al.* [STAR Collaboration], arXiv: 1204.4244.
 98 [4] B. I. Abelev *et al.*, Phys. Rev. Lett. **98**, 192301 (2007).
 99 [5] M. Shao *et al.*, Nucl. Instrum. Methods A **499**, 624 (2003).
 100 [6] J. Adams *et al.*, Phys. Rev. Lett. **94**, 062301 (2005).
 101 [7] J. Adams *et al.* [STAR Collaboration], Phys. Rev. Lett. **91**, 172302 (2003).
 102 [8] R. Vogt, private communication, (2012).
 103 [9] M. Honda *et al.*, Phys. Rev. Lett. **70**, 525 (1993).
 104 [10] M. He, R. J. Fries, R. Rapp, arXiv: 1204.4442.
 105 [11] P. B. Gossiaux, J. Aichelin, M. Bluhm, T. Gousset, M. Nahrgang, S. Vogel, K. Werner, arXiv: 1207.5445.
 106 [12] R. Vogt, Eur.Phys.J.ST **155** 213 (2008).
 107 [13] Z. Xu *et al.*, J. Phys. G **32**, S571 (2006).